Supplementary information for:

A general strategy based on the self-evolution of building blocks for the construction of one-dimensional hierarchically superstructured TiO_2 fibres

Yun Wang,[a,b] Haibo Huang,[c] Daoguang Du,[a] Yanfeng Dong,[a] Zhongmin Feng,[a] Yuanpeng Wang,[d] Ting Sun,*[a] and Yan Xu*[b]*

[a] College of Sciences, Northeastern University, 3-11, Wenhua Road, Shenyang, Liaoning, 110819, China. E-mail: sun1th@163.com

[b] State Key Lab of Inorganic Synthesis and Preparative Chemistry, Jilin University, 2699 Qianjin Street, Changchun, 130012, China. Tel: 86 431 85168607; E-mail: yanxu@jlu.edu.cn

[c] Dalian National Laboratory for Clean Energy, Dalian Institute of Chemical Physics, Chinese Academy of Sciences, 457 Zhongshan Road, Dalian, 116023, China.

[d] College of Food Science, Shenyang Agricultural University, 120, Dongling Road, Shenyang, Liaoning, 110866, China. E-mail: wangypchem@163.com

Experimental

Materials

Polyvinyl pyrrolidone (PVP, Mw ≈ 1 300 000, Aldrich), anhydrous ethanol (EtOH), N, N-dimethylformamide (DMF), acetylacetone (Acac), $Pb(OAc)_2•3H_2O$, $Zn(OAc)_2•2H_2O$, $Cu(OAc)_2•H_2O$, titanium (IV) butoxide (TBT, Guangfu Fine Chemicals), sodium hydroxide (NaOH), and hydrochloric acid (HCl, Beijing Chemicals) were used. All chemicals were used as received.

Preparation of the amorphous metal-doped TiO_2 template precursor

The amorphous metal-doped TiO_2 template fibres were obtained from the well-known electrospinning process, followed by a controlled heat treatment. For fabrication of the amorphous Pb-doped TiO_2 template precursor, PVP (0.8 g), $Pb(OAc)_2•3H_2O$ (0.2 g) and TBT (2.8 g) were added to a mixture solution of EtOH (4.0 g), Acac (0.2 g) and DMF (1.5 g), and stirred for 24 h to form a homogeneous solution. The solution was fed through syringe with stainless steel spinneret (18 G, inner diameter: 0.84 mm). A voltage of 15 kV was applied and the electrospun fibres were collected on grounded aluminium foil. Then, the amorphous Pb-doped TiO_2 template precursor were obtained after calcinating the electrospun PVP/TiO_2 fibres at 410 °C for 6 h under air atmosphere at a rate of 5 °C min^{-1}.

The amorphous Zn-doped TiO_2 template precursor was fabricated with similar process with the raw materials of PVP (0.8 g), $Zn(OAc)_2•2H_2O$ (0.2 g) and TBT (2.8 g)

were added to a mixture solution of EtOH (4.0 g) and DMF (1.5 g). The calcination temperature was 405 °C.

The amorphous Cu-doped TiO_2 template precursor was fabricated with similar process with the raw materials of PVP (0.8 g), $Cu(OAc)_2 \cdot H_2O$ (0.1 g) and TBT (2.9 g) were added to a mixture solution of EtOH (5.5 g). The calcination temperature was 340 °C.

The amorphous TiO_2 template precursor without metal-doped was fabricated with similar process with the raw materials of PVP (0.8 g), and TBT (3.0 g) were added to a mixture solution of EtOH (5.0 g) and HOAc (1.0 g). The calcination temperature was 350 °C

Preparation of the 1D-HS metal-doped titanate and TiO_2-carbon materials

The preparation of the 1D-HS metal-doped titanate was carried out under alkali conditions. Typically, 40 mg of the amorphous metal-doped TiO_2 template precursor were immersed in 1 M NaOH aqueous solution, and transferred into a polytetrafluoroethylene (Teflon)-lined stainless-steel autoclave with a total volume of 20 mL. Then, the autoclave was sealed and heated to 150 °C for 24 h. The products were washed repeatedly with DI water till pH~7, and the 1D-HS metal-doped titanate were prepared.

The 1D-HS metal-doped TiO_2-carbon materials were prepared as follows: After the hydrothermal treatment, the Na^+ ions contained in the 1D-HS metal-doped titanate were removed by ion exchanging with an HCl (0.1 M) aqueous solution for 24 h, and washing repeatedly with DI water till pH~7. Then, the samples were oven-dried at 60 °C, and

calcined at 600 °C for 2 h under nitrogen atmosphere to obtain the 1D-HS metal-doped TiO_2-carbon materials.

Preparation of the 1D-HS Pb-doped TiO_2-carbon/S hybrid

S loaded 1D-HS Pb-doped TiO_2-carbon materials were obtained as follows: the 1D-HS Pb-doped TiO_2-carbon were grinded with sublimed S, and then heated at 155 °C for 12 h in sealed container with Ar atmosphere, the load mass of S is about 77.4 wt%.

Characterization

Field-emission scanning electron microscopy (FE-SEM) was taken on JEOL JSM 6700F. Transmission electron microscopy (TEM) was recorded on FEI Tecnai G2S-Twin with an EDS attachment. X-ray diffraction measurements (XRD) were performed on Rigaku D/MAXrB. Nitrogen adsorption-desorption isotherms were carried out at 77 K using Micromeritics ASAP 2420M system. All the samples were degassed at 200 °C for 10 h prior to measurement. Brunauer-Emmett-Teller (BET) surface area and pore size distributions were calculated using the Barret-Joyner-Halenda (BJH) model.

Electrochemical measurements

To prepare the composite cathode, the 1D-HS Pb-doped TiO_2-carbon/S hybrid materials (70 wt %), Poly(vinylidenedifuoride) (PVDF, 10 wt %) and Super P (20 wt %) were dispersed in N-methylpyrrolidone (NMP, electronic grade, Aladdin) to form a stable viscous slurry, and then the slurry was casted onto the aluminium foil and followed by drying in vacuum for 12 h at 90 °C. The CR2016 coin cells were assembled using Celgard 2300 membrane as separator and Li foil as anode. 1 M lithium bis(tri-trifluoromethanesulfonyl)imide (LiTFSI) in a mixed solution of 1,3-dioxolane (DOL) and

1,2-dimethoxyethane (DME) (volume ratio 1:1) containing 1.0 wt % $LiNO_3$ was used as the electrolyte. The galvanostatic charge-discharge tests were performed on a LAND testing system at room temperature in the voltage range of 1.7-2.8 V (versus Li/Li^+), and the specific capacity is calculated based on the mass of S.

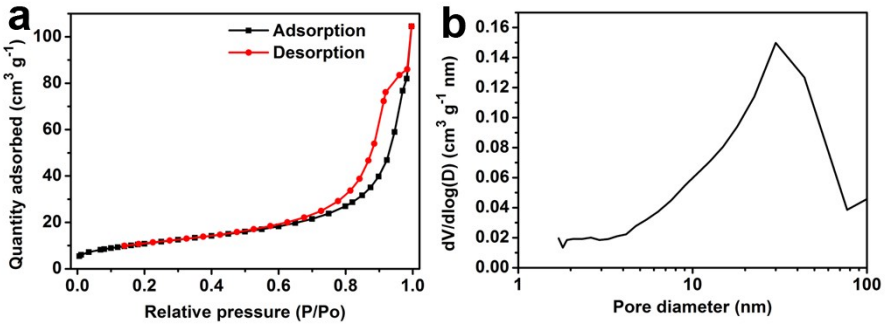

Fig. S1 (a) N_2 adsorption–desorption isotherm and (b) the BJH pore size distribution plot of the the pomegranate-like amorphous Pb-doped TiO_2 precursor.

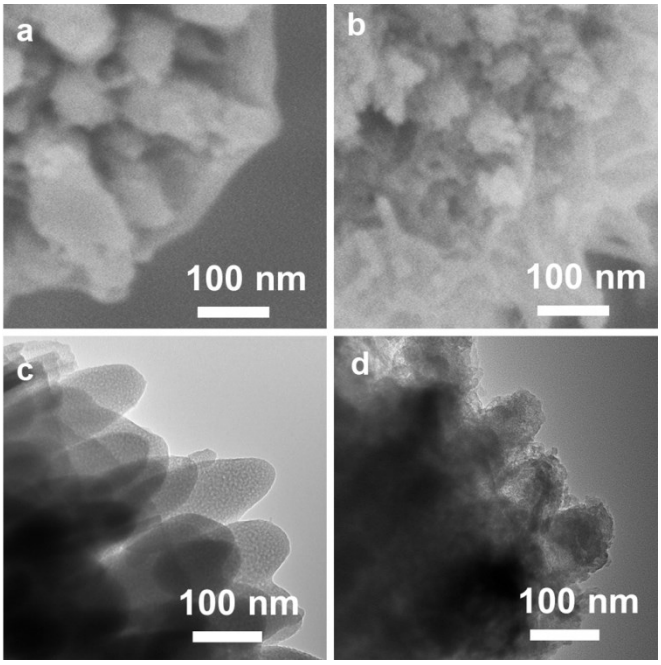

Fig. S2 (a) and (c) high-magnification SEM and TEM images of the cross section of the pomegranate-like amorphous metal-doped TiO_2 precursor composed of nanospheres in tube; (b)

and (d) high-magnification SEM and TEM images of the cross section of the intermediate product obtained by hydrothermal treating at 150 °C for 15 min. The results indicate that the titanate first nucleates *in situ* and grows on the surface of each building blocks. The chemical reaction continues from outside to inside of the each building blocks.

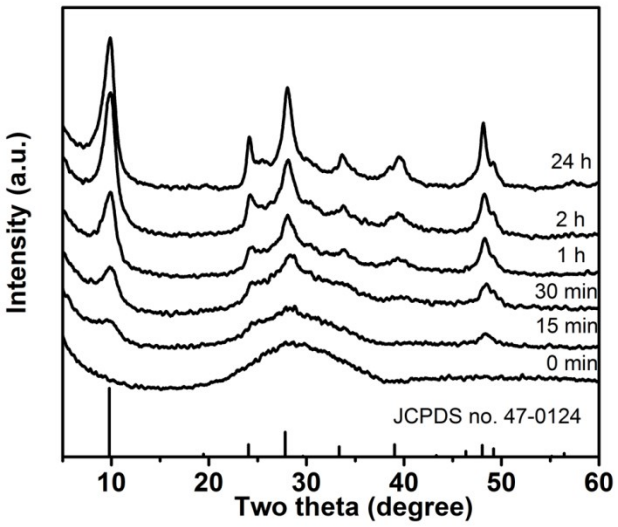

Fig. S3 XRD patterns of time-dependent evolution of the 1D-HS Pb-doped titanate obtained for different hydrothermal time. The peaks at 9.8°, 24.1°, 27.8°, 33.4°, 39° and 48°, which are indexed as titanate crystal planes of (200), (110), (310), (301), (501) and (020) ($Na_{2-x}H_xTi_2O_4(OH)_2$, JCPDS, no. 47-0124).

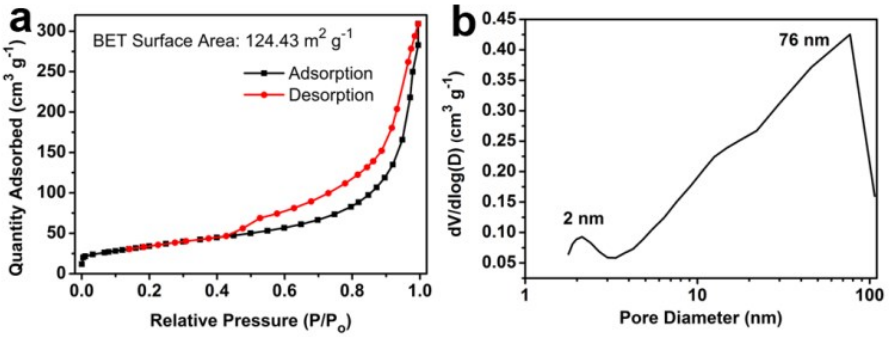

Fig. S4 (a) N_2 adsorption–desorption isotherm and (b) the BJH pore size distribution plot of the 1D-HS Pb-doped titanate.

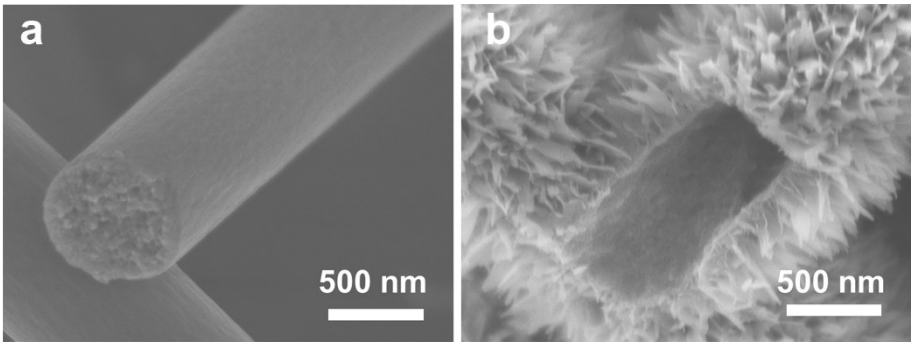

Fig. S5 (a) SEM image of the amorphous TiO_2 precursor without metal-doped; (b) SEM image of the resultant hierarchical tubular titanate.

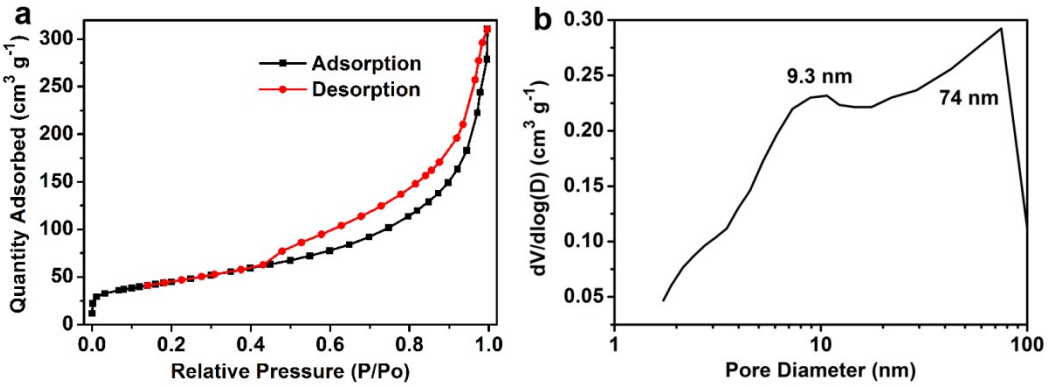

Fig. S6 (a) N_2 adsorption–desorption isotherm and (b) the BJH pore size distribution plot of the 1D-HS Pb-doped TiO_2-carbon materials.

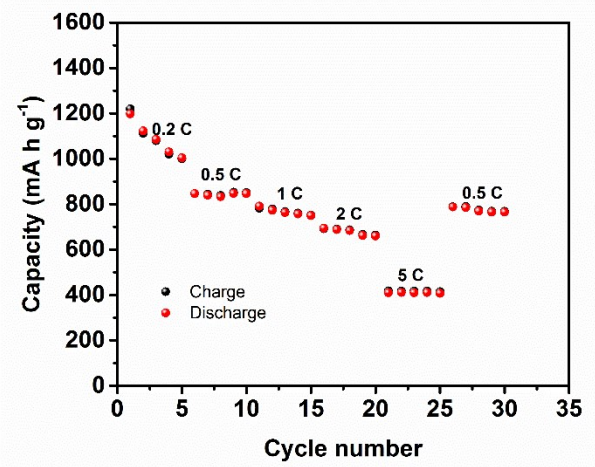

Fig. S7 Rate capacity of the 1D-HS Pb-doped TiO_2-carbon/S electrode.

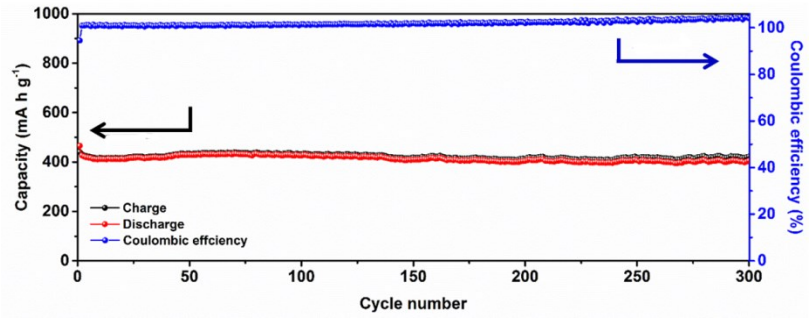

Fig. S8 The cycling stability and coulombic efficiency of the 1D-HS Pb-doped TiO_2-carbon/S materials at 5 C.

Table S1 Comparison of the cycle performances of various sulfur electrode composites reported in the recent literatures.

Electrode composites	Sulfur content (wt%)	Current density (1C=1675 mA h g^{-1})	Cycle performances (mA h g^{-1})	Capacity fading rate per cycle	Reference/ Publish date
Mesoporous TiO_2	70	1 C	578 (100 cycles)	0.110%	[1]/2013
Ordered mesoporous carbon	60	5.8 C	274 (400 cycles)	0.117%	[2]/2011
Pea-pod-like nitrogen-doped hollow porous carbon	65.4	2 C	604 (1500 cycles)	0.024%	[3]/2018
Porous carbon@Ti_4O_7 nanoparticle	77	4 C	352 (1000 cycles)	0.044%	[4]/2018
TiO_2@Hollow carbon nanoballs	73	0.5 C	508 (600 cycles)	0.069%	[5]/2019
Hollow multi-shelled TiO_{2-x}	56	0.5 C	713 (1000 cycles)	0.021%	[6]/2019
TiO_2/TiC Composite	55	0.2 C	440 (400 cycles)	0.124%	[7]/2019
Hierarchically porous TiN	72	5 C	586 (1000 cycles)	0.016%	[8]/2019

Co within mesoporous carbon	63	0.5 C	837 (300 cycles)	0.086%	[9]/2019
Carbon cloth@CoP/carbon	78	2 C	833 (600 cycles)	0.016%	[10]/2019
Hierarchical nitrogen-doped carbon nanotubes@MoS_2	70	2 C	758 (150 cycles)	0.049%	[11]/2019
FeCoNi alloy doped graphene nanotube	56	1 C	554 (500 cycles)	0.080%	[12]/2019
Hierarchical porous hollow carbon nanospheres	75	1 C	418 (1000 cycles)	0.044%	[13]/2020
hierarchically porous PANI/MnO_2	60.2	2 C	640 (500 cycles)	Not given	[14]/2020
N-doped carbon/MoS_3 nanoboxes	70	0.5 C	752 (500 cycles)	0.075%	[15]/2020
Porous carbon nanosheet-TiO_2	70	0.5 C	718 (300 cycles)	0.063%	[16]/2020
1D-HS Pb-doped TiO_2 fibers	**77.4**	**5 C**	**405 (300 cycles)**	**0.043%**	**This Work**

Reference:

[1] B. Ding, L. Shen, G. Xu, P. Nie and X. Zhang, Electrochimica Acta, 2013, 107, 78-84.

[2] S.-R. Chen, Y.-P. Zhai, G.-L. Xu, Y.-X. Jiang, D.-Y. Zhao, J.-T. Li, L. Huang and S.-G. Sun, Electrochimica Acta, 2011, 56, 9549-9555.

[3] W. Yao, C. Chu, W. Zheng, L. Zhan and Y. Wang, Journal of Materials Chemistry A, 2018, 6, 18191-18205.

[4] A. Chen, W. Liu, H. Hu, T. Chen, B. Ling and K. Liu, Journal of Materials Chemistry A, 2018, 6, 20083-20092.

[5] H. Gu, H. Wang, R. Zhang, T. Yao, T. Liu, J. Wang, X. Han and Y. Cheng, Industrial & Engineering Chemistry Research, 2019, 58, 18197-18204.

[6] E. H. M. Salhabi, J. Zhao, J. Wang, M. Yang, B. Wang and D. Wang, Angewandte Chemie International Edition, 2019, 58, 9078-9082.

[7] X. Lang, Y. Zhao, K. Cai, L. Li, D. Chen and Q. Zhang, Energy Technology, 2019, 7, 1900543.

[8] W.-G. Lim, C. Jo, A. Cho, J. Hwang, S. Kim, J. W. Han and J. Lee, Advanced Materials, 2019, 31, 1806547.

[9] J. Xie, B.-Q. Li, H.-J. Peng, Y.-W. Song, M. Zhao, X. Chen, Q. Zhang and J.-Q. Huang, Advanced Materials, 2019, 31, 1903813.

[10] Z. Wang, J. Shen, J. Liu, X. Xu, Z. Liu, R. Hu, L. Yang, Y. Feng, J. Liu, Z. Shi, L. Ouyang, Y. Yu and M. Zhu, Advanced Materials, 2019, 31, 1902228.

[11] W. Yang, W. Yang, L. Dong, X. Gao, G. Wang and G. Shao, Journal of Materials Chemistry A, 2019, 7, 13103-13112.

[12] O. Ogoke, S. Hwang, B. Hultman, M. Chen, S. Karakalos, Y. He, A. Ramsey, D. Su, P.

Alexandridis and G. Wu, Journal of Materials Chemistry A, 2019, 7, 13389-13399.

[13] Z. Yu, M. Liu, D. Guo, J. Wang, X. Chen, J. Li, H. Jin, Z. Yang, X. a. Chen and S. Wang, Angewandte Chemie International Edition, 2020, 59, 6406-6411.

[14] Y. Zhang, X. Liu, L. Wu, W. Dong, F. Xia, L. Chen, N. Zhou, L. Xia, Z.-Y. Hu, J. Liu, H. S. H. Mohamed, Y. Li, Y. Zhao, L. Chen and B.-L. Su, Journal of Materials Chemistry A, 2020, 8, 2741-2751.

[15] L. Guo, J. Yu, J. Xiao, A. Li, Z. Yang, L. Zeng, Q. Zhang and Y. Zhu, Angewandte Chemie International Edition, 2020, DOI: 10.1002/anie.202004914.

[16] Y. Jiang, Y. Deng, B. Zhang, W. Hua, X. Wang, Q. Qi, Q. Lin and W. Lv, Nanoscale, 2020. DOI: 10.1039/D0NR02607G